

Quantum limits of ballistic electrical and thermal resistances of semiconductors

Cite as: AIP Advances 16, 025331 (2026); doi: 10.1063/5.0306761

Submitted: 30 December 2025 • Accepted: 27 January 2026 •

Published Online: 18 February 2026



Alice Ho,¹ Jashan Singhal,^{1,a)} Deji Akinwande,² Huili G. Xing,^{1,3,4} and Debdeep Jena^{1,3,4,b)}

AFFILIATIONS

¹School of Electrical and Computer Engineering, Cornell University, Ithaca, New York 14853, USA

²Department of Electrical and Computer Engineering, University of Texas at Austin, Austin, Texas 78712, USA

³Department of Materials Science and Engineering, Cornell University, Ithaca, New York 14853, USA

⁴Kavli Institute at Cornell for Nanoscale Science, Cornell University, Ithaca, New York 14853, USA

^{a)}Now at: Intel Corporation, Hillsboro, Oregon, USA

^{b)}Author to whom correspondence should be addressed: djena@cornell.edu

ABSTRACT

The importance of electrical contact resistance and thermal boundary resistance has increased dramatically as devices are scaled to atomic limits. The use of a rich range of materials with various bandstructures (e.g., parabolic and conical) and in geometries exploiting various dimensionalities (e.g., 1D wires, 2D sheets, and 3D bulk) will increase in the future. Here, we derive a single general expression for the quantum limit of electrical contact resistivity for various bandstructures and all dimensions. A corresponding result for the quantum limit of thermal boundary resistance is also derived. These results will be useful to quantitatively co-design, benchmark, and guide the lowering of electrical and thermal boundary resistances for energy efficient devices.

© 2026 Author(s). All article content, except where otherwise noted, is licensed under a Creative Commons Attribution (CC BY) license (<https://creativecommons.org/licenses/by/4.0/>). <https://doi.org/10.1063/5.0306761>

In studies of semiconductors with parabolic bandstructures, Maasen *et al.*¹ and Barasker *et al.*² derived separate expressions for the quantum limits of electrical contact resistivity for $d = 1, 2$, and 3 dimensions.^{3–7} Recently, Singhal and Jena (SJ) derived a *single* unified expression for particle, charge, and heat currents in the quantum limit for various bandstructures and dimensions.⁸ Using Ref. 8, in this letter, we derive a *single* unified expression for the quantum limit of electrical contact resistivity for any dimension ($d = 1, 2, 3$) and for two bandstructures: parabolic $E(k) = \hbar^2 k^2 / 2m^*$ and conical $E(k) = \hbar v_F k$, as indicated in Figs. 1(a)–1(e). The general results derived in this work apply to anisotropic bands of each type in all dimensions and temperatures. A general quantum limit of thermal boundary resistance is also derived using Ref. 8. The results address the increased need of co-designing electro-thermal phenomena in devices in their atomic limits, both at room temperature and in the cryogenic limit.

The unified SJ ballistic equation for particle, charge, and energy currents $J = g \sum_k v(k)^a E(k)^b f(k)$, a sum over states k of group velocity $v(k)$, energy $E(k)$, and occupation $f(k)$ in the ballistic limit is derived in Ref. 8 to be

$$J_{d,t}^{a,b} = \frac{g}{\lambda^d \beta^b} \cdot \left(\frac{\lambda_1}{\hbar \beta} \right)^a \cdot C_{d,t}^{a,b} \cdot F_j^\pm(\eta), \quad (1)$$

where λ is the de-Broglie wavelength of electrons (or phonons), \hbar is Planck's constant, $\beta = 1/(k_b T)$, and $F_j^\pm(\eta) = \frac{1}{\Gamma(j+1)} \int_0^\infty dx \frac{x^j}{\exp[x-\eta] \pm 1}$ is the Fermi-Dirac (+) or Bose-Einstein (−) integral. All terms and units of Eq. (1) are explicitly defined in Ref. 8 for parabolic ($t = 2$) and conical ($t = 1$) energy dispersions.

For charge current ($a = 1$ and $b = 0$) of *fermions*, Eq. (1) is

$$J_{d,t}^{1,0}(v) = g \cdot \frac{q}{\hbar} \cdot \frac{\lambda_1}{\lambda^d} \cdot \frac{\Gamma(r+1)}{\Gamma\left(\frac{d+1}{2}\right)} \cdot \left[\frac{F_r^+(\eta) - F_r^+(\eta-v)}{\beta} \right], \quad (2)$$

where $r = (d-1)/t$, q is the electron charge, and $g = g_s g_v$ is the product of the spin degeneracy g_s and the valley degeneracy g_v . λ_1 is the de-Broglie wavelength in the direction of net current flow⁹ and $\Gamma(\dots)$ is the gamma function. $\eta = \beta E_F$ is the dimensionless chemical potential and $v = \beta q V$ is the dimensionless voltage for which the fermionic current flows in response. The quantum contact conductivity, $\sigma_c^d = \lim_{V \rightarrow 0} J_{d,t}(v)/V$,

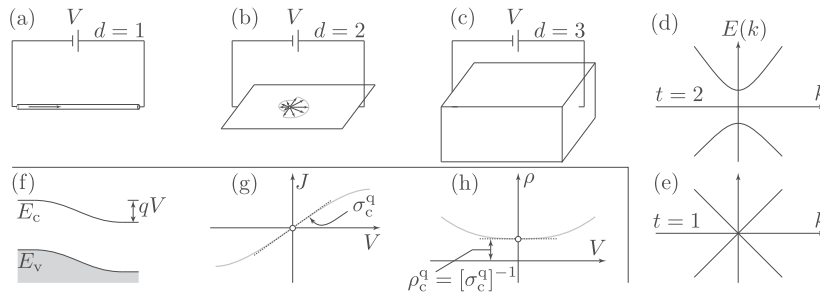


FIG. 1. Schematic representation of (a) 1D, (b) 2D, and (c) 3D channels with (d) parabolic bands with $t = 2$ and (e) linear bands with $t = 1$ energy bandstructure, which is written as $E(k) = [\sum_{i=1}^d (\alpha_i k_i)^2]^{\frac{1}{2}}$, where $\alpha_i = \hbar v_{Fi}$ for linear and $\alpha_i = \hbar/\sqrt{2m_i}$ for parabolic bands. The schematic energy band diagram in panel (f) indicates the current response $J - V$ curve of panel (g) and results in the contact resistivity in panel (h).

$$\sigma_c^q = g \cdot \frac{q^2}{h} \cdot \frac{\lambda_1}{\lambda^d} \cdot \frac{\Gamma(r+1)}{\Gamma(\frac{d+1}{2})} \cdot \lim_{v \rightarrow 0} \left[\frac{F_r^+(\eta) - F_r^+(\eta-v)}{v} \right]_{\partial F_r^+(\eta)/\partial \eta = F_{r-1}^+(\eta)}$$

$$\Rightarrow \sigma_c^q = g \cdot \frac{q^2}{h} \cdot \frac{\lambda_1}{\lambda^d} \cdot \frac{\Gamma(\frac{d-1}{2} + 1)}{\Gamma(\frac{d+1}{2})} \cdot F_{\frac{d}{2}-1}^+(\eta), \quad (3)$$

and the mobile fermion density,

$$n_{d,t} = 2J_{d,t}^{0,0} = \frac{2g}{\lambda^d} \cdot \frac{\Gamma(\frac{d}{2})}{t\Gamma(\frac{d}{2})} \cdot F_{\frac{d}{2}-1}^+(\eta), \quad (4)$$

form a pair of *exact* closed-form analytical expressions of measurable quantities for all dimensions and temperatures. Combining Eq. (3) with Eq. (4) helps express the exact generalized quantum contact conductivity limit as

$$\sigma_c^q = \left[g^{\frac{1}{d}} \cdot \frac{q^2}{h} \cdot \frac{\lambda_1}{\lambda} \cdot (n_{d,t})^{\frac{d-1}{d}} \right] \cdot H_{d,t}(\eta), \quad (5)$$

where the unitless factor $H_{d,t}(\eta)$ is

$$H_{d,t}(\eta) = \frac{\Gamma(\frac{d-1}{2} + 1)}{\Gamma(\frac{d+1}{2})} \cdot \left[\frac{t\Gamma(\frac{d}{2})}{\Gamma(\frac{d}{2})} \right]^{\frac{d-1}{d}} \cdot \frac{F_{\frac{d}{2}-1}^+(\eta)}{\left[F_{\frac{d}{2}-1}^+(\eta) \right]^{\frac{d-1}{d}}}. \quad (6)$$

Low-resistance contacts are made to degenerately doped materials for which $\eta \gg +1$ and the Fermi-Dirac integrals are $F_j^+(\eta) \approx \eta^{j+1}/\Gamma(j+2)$. Then, $H_{d,t}(\eta \rightarrow \infty) = [\Gamma(\frac{d+2}{2})]^{(d-1)/d}/\Gamma(\frac{d+1}{2})$, independent of both η and the bandstructure t , depending only on d . The degenerate limit of the quantum limit of contact resistance for isotropic bandstructure ($\lambda_1 = \lambda$) from Eq. (5) written explicitly then is

$$\rho_c^q = (\sigma_c^q)^{-1} \approx \frac{h}{q^2} \cdot \frac{1}{(g_s g_v)^{\frac{1}{d}}} \cdot \frac{\Gamma(\frac{d+1}{2})}{[\Gamma(\frac{d+2}{2})]^{\frac{d-1}{d}}} \cdot \frac{1}{(n_d)^{\frac{d-1}{d}}}, \quad (7)$$

which is universal and valid for both parabolic ($t = 2$) and conical ($t = 1$) bandstructures for all dimensions d . To a good approximation, $[\Gamma(\frac{d+2}{2})]^{(d-1)/d}/\Gamma(\frac{d+1}{2}) \approx d^{1/6}$ for $d = 1, 2, 3$. This reveals that

the generalized degenerate limit of the quantum limit of electrical contact conductivity is the rather simple relation,

$$\sigma_c^q \approx (g_s g_v)^{\frac{1}{d}} \cdot \frac{q^2}{h} \cdot d^{\frac{1}{6}} \cdot (n_d)^{\frac{d-1}{d}}. \quad (8)$$

The generalized result Eq. (5) of the electronic quantum contact conductance and its degenerate limit relations Eqs. (7) and (8) are the main results of this work. The ratio of gamma functions in Eq. (6) is unity for parabolic bandstructure ($t = 2$), and the exact generalized quantum conductivity for this case is

$$\sigma_c^q = (g_s g_v)^{\frac{1}{d}} \cdot \frac{q^2}{h} \cdot \frac{\lambda_1}{\lambda} \cdot (n_d)^{\frac{d-1}{d}} \cdot \frac{F_{\frac{d-3}{2}}^+(\eta)}{\left[F_{\frac{d}{2}-1}^+(\eta) \right]^{\frac{d-1}{d}}}. \quad (9)$$

Figure 1(b) schematically indicates the group velocity vectors of carriers. The right-moving states are in equilibrium with the left electrode whose chemical potential is maintained at an energy qV higher by the voltage source than the right electrode, with which the left-moving states are in equilibrium. Figure 1(f) indicates an energy band diagram, and Fig. 1(g) shows the current–voltage response whose $V \rightarrow 0$ slope is the quantum limit of conductivity σ_c^q given by Eq. (5). The $V \rightarrow 0$ limit of electrical resistivity $\rho = 1/(\partial J/\partial V)$ shown in Fig. 1(h) is the quantum limit of the contact resistance, $\rho_c^q = 1/\sigma_c^q$.

Equation (5) indicates a transition from $\rho_c^q \propto n_d^{-1}$ for all d for low n_d to $\rho_c^q \propto n_d^{-(d-1)/d}$ for high n_d . While Eqs. (7) and (8) are applicable in desired ultralow resistance ohmic contacts due to high carrier concentrations, for low carrier density contacts, Eq. (5) must be used. Figure 2 shows the calculated quantum limits of contact resistance as a function of the carrier densities using Eq. (5) as solid lines and its degenerate limit using Eq. (8) as dashed lines. Figure 2(a) for a $d = 1$ channel shows that in the degenerate limit, the quantum limit of the 1D contact resistance is the Landauer or Sharvin limit, which also appears experimentally in quantized conductance, the integer quantum Hall effect, and the conductance per subband in metallic single-wall carbon nanotubes.¹⁰

Although Eq. (8) shows that for $d = 1$, $\rho_c^q \rightarrow h/(gq^2)$ in the degenerate limit is independent of the 1D carrier density, from Eq. (5) and Fig. 2(a), the quantum contact resistance limit increases inversely with the carrier density $\rho_c^q \propto 1/n_{1d}$ in the non-degenerate

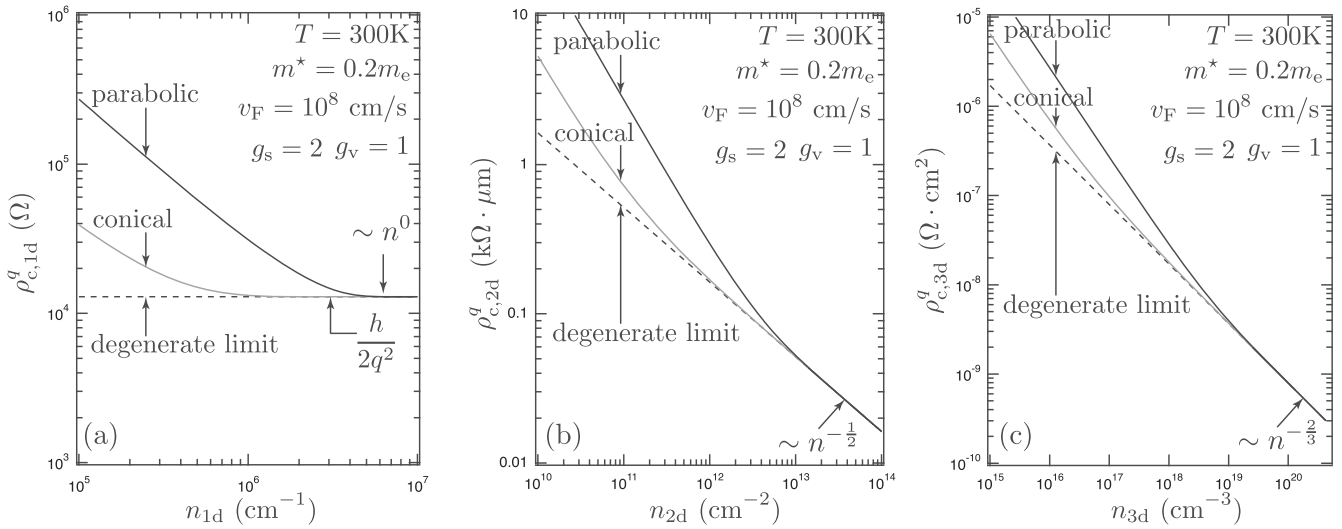


FIG. 2. Quantum limit of electrical contact resistance for (a) 1D, (b) 2D, and (c) 3D conducting channels. Each of the three plots compare values at $T = 300\text{ K}$ for parabolic bandstructure with $m^* = 0.2m_e$ represented by the thick solid lines, conical bands with Fermi velocity $v_F = 10^8\text{ cm/s}$ represented by the thin solid gray lines, each with spin degeneracy $g_s = 2$ and valley degeneracy $g_v = 1$. The degenerate limit from Eq. (8) is indicated by the dashed line.

limit, for both parabolic and conical bandstructures. Thus, for a doubly degenerate spin 1D channel with a parabolic bandstructure with $m^* = 0.2m_e$ at 300 K , $\rho_c^q = h/(2q^2) = 12.6\text{ k}\Omega$ for $n_{1d} > 5 \times 10^6/\text{cm}$, which increases to $\rho_c^q \approx 30\text{ k}\Omega$ for $n_{1d} = 10^6/\text{cm}$, at which carrier density for the conical bandstructure with $v_F = 10^8\text{ cm/s}$ and the contact resistance stays at $\rho_c^q = 12.6\text{ k}\Omega$. This comparison shows that care must be exercised in using the degenerate limit result of Eq. (8), indicated by the dashed line shown in Fig. 2(a), because it is valid only in the degenerate limit, whereas Eq. (5) is always valid.

The points made for the quantum limit of contact resistance for the 1D case shown in Fig. 2(a) are reinforced in Fig. 2(b) for 2D channels and in Fig. 2(c) for 3D channels. The degenerate quantum limit of the contact resistance goes as $\sim n_d^{-(d-1)/d}$ according to Eq. (7). Therefore, while for $d = 1$, this has no dependence on the 1D carrier density ($\rho_c^q \sim n_{1d}^0$), Fig. 2(b) indicates that for $d = 2$, the dependence is $\rho_c^q \sim n_{2d}^{-1/2}$, and Fig. 2(c) shows that for $d = 3$, it is $\rho_c^q \sim n_{3d}^{-2/3}$. In the non-degenerate limit at low carrier concentrations, all quantum limited contact resistances follow a universal dependence on the carrier density of $\rho_c^q \sim n_d^{-1}$, both for parabolic and conical bandstructures, although the precise values may differ based on the bandstructure parameters m^* for parabolic and v_F for conical. This dependence changes to the universal dependence of $\sim n_d^{-(d-1)/d}$ in the degenerate limit, where the bandstructure parameters m^* for parabolic and v_F for conical do not matter anymore.

What is not explicitly shown in Fig. 2 is the dependence of ρ_c^q on the spin and valley degeneracies (g_s, g_v) of the bandstructure and anisotropies. Equations (5) and (7) show that these properties do have an effect on the precise values of ρ_c^q at all carrier densities, but do not change the asymptotic power law dependencies on the carrier densities at the two extremes. Figure 2 shows that for semiconductor channels in the degenerate limit, the lowest

contact resistances for each valley with $g_s = 2$ are $\sim 12.6\text{ k}\Omega$ for 1D, $\sim 0.05\text{ k}\Omega \cdot \mu\text{m}$ ($\approx 0.05\text{ }\Omega \cdot \text{mm} = 50\text{ }\Omega \cdot \mu\text{m}$) for $n_{2d} \sim 10^{13}/\text{cm}^2$, and $\sim 8 \times 10^{-10}\text{ }\Omega \cdot \text{cm}^2$ for $n_{3d} \sim 10^{20}/\text{cm}^3$.

As emphasized in Refs. 1, 2, 11, and 12, because the quantum limit formulas here assume a unity transmission coefficient, the presence of tunneling barriers increase the actual ρ_c from the limits ρ_c^q derived and plotted in Fig. 2. The conical bandstructure discussed here is not limited to graphene-like Dirac cone bandstructures because the bandstructure of narrow bandgap semiconductor far from the band edges approaches linear $E(k)$ dependence.¹³ A detailed comparison of current state-of-the-art experimental contact resistances for various materials of different dimensionalities, anisotropies, and bandstructures will be presented in a separate comprehensive article expanding the results discussed in this letter.

To obtain the generalized quantum limit of the thermal boundary resistance,¹⁴⁻¹⁶ the heat current requires higher moment terms with $(a, b) = (1, 1)$ in the SJ ballistic Eq. (1). The general expression in d -dimensions for the ballistic thermal boundary resistance is obtained from the heat current $Q_{d,t} = J_{d,t}^{1,1} - \mu J_{d,t}^{1,0}$ flowing from an electrode at chemical potential μ and temperature T . The heat current is carried primarily by phonons (=bosons) in a semiconductor. Then, the chemical potential $\mu = 0$ and the low-energy dispersion $\omega(k) = vk$ for each acoustic phonon branch with $t = 1$ is characterized by a sound velocity v of that branch.

The heat current density per acoustic phonon branch is then

$$Q_d = \frac{g\pi^{\frac{d-1}{2}} k_b^{d+1}}{h^d v^{d-1}} \cdot \frac{\Gamma(d+1)}{\Gamma(\frac{d+1}{2})} \cdot F_d^-(0) \cdot T^{d+1}, \quad (10)$$

where the Bose-Einstein integral $F_d^-(\dots)$ is related to the Riemann zeta function $\zeta(\dots)$ via $F_d^-(0) = \zeta(d+1)$. The quantum limit of the thermal boundary conductance $\kappa_c^q = \partial Q_d / \partial T$ in d -dimensions for each phonon branch then becomes

TABLE I. Quantum limits of electrical contact resistance and thermal boundary resistance in various dimensions.

	1D	2D	3D
σ_c^q (parabolic, exact)	$\frac{q^2}{h} (g_s g_v) F_{-1}^+(\eta)$	$\frac{q^2}{h} (g_s g_v)^{\frac{1}{2}} \frac{\lambda_1}{\lambda} (n_{2d})^{\frac{1}{2}} \frac{F_{-\frac{1}{2}}^+(\eta)}{[F_0^+(\eta)]^{\frac{1}{2}}}$	$\frac{q^2}{h} (g_s g_v)^{\frac{1}{3}} \frac{\lambda_1}{\lambda} (n_{3d})^{\frac{2}{3}} \frac{F_0^+(\eta)}{[F_{\frac{1}{3}}^+(\eta)]^{\frac{2}{3}}}$
σ_c^q (conical, exact)	$\frac{q^2}{h} (g_s g_v) F_{-1}^+(\eta)$	$\frac{q^2}{h} (g_s g_v)^{\frac{1}{2}} \frac{\lambda_1}{\lambda} (n_{2d})^{\frac{1}{2}} \sqrt{\frac{2}{\pi}} \frac{F_0^+(\eta)}{[F_{+1}^+(\eta)]^{\frac{1}{2}}}$	$\frac{q^2}{h} (g_s g_v)^{\frac{1}{3}} \frac{\lambda_1}{\lambda} (n_{3d})^{\frac{2}{3}} \frac{\pi^{\frac{1}{2}}}{4} \frac{F_{+1}^+(\eta)}{[F_{+2}^+(\eta)]^{\frac{2}{3}}}$
ρ_c^q (degenerate)	$\frac{h}{q^2} \frac{1}{g_s g_v}$	$\frac{h}{q^2} \sqrt{\frac{\pi}{4 g_s g_v n_{2d}}}$	$\frac{h}{q^2} \left(\frac{16}{9 \pi g_s g_v (n_{3d})^2} \right)^{\frac{1}{3}}$
κ_c^q	$\frac{\pi^2}{3} \frac{k_b^2}{h} T$	$12 \zeta(3) \frac{k_b^3}{h^2 v} T^2$	$\frac{4 \pi^5}{15} \frac{k_b^4}{h^3 v^2} T^3$
$\frac{\kappa_c^q \rho_c^q (\text{deg.})}{T^d}$	$\frac{\pi^2}{3 g_s g_v} \frac{k_b^2}{q^2}$	$6 \zeta(3) \sqrt{\frac{\pi}{g_s g_v n_{2d}}} \frac{k_b^3}{h v q^2}$	$\frac{4 \pi^5}{15} \left(\frac{16}{9 \pi g_s g_v (n_{3d})^2} \right)^{\frac{1}{3}} \frac{k_b^4}{h^2 v^2 q^2}$

$$\kappa_c^q = \frac{\pi^{\frac{d-1}{2}} \cdot \zeta(d+1) \cdot \Gamma(d+2)}{\Gamma(\frac{d+1}{2})} \cdot \frac{g k_b^{d+1} T^d}{h^d v^{d-1}} \quad (11)$$

Since $\zeta(s) = \sum_{u=1}^{\infty} 1/u^s$, we have $\zeta(2) = \pi^2/6$ for $d = 1$, $\zeta(3) \approx 1.202$ for $d = 2$, and $\zeta(4) = \pi^4/90$ for $d = 3$. The resulting expressions for the quantum limit of the thermal boundary conductance are, therefore, $\kappa_c^q(1D) = \frac{\pi^2 k_b^2}{3h} T$, $\kappa_c^q(2D) = \frac{12 \zeta(3) k_b^3}{h^2 v} T^2$, and $\kappa_c^q(3D) = \frac{4 \pi^5 k_b^4}{15 h^3 v^2} T^3$. Equation (11) is thus the generalized Kapitza conductance for d - dimensions. Example values of this limit of thermal boundary conductances at $T = 300$ K for 1D is $\kappa_c^q(1D) \approx 2.8 \times 10^{-10}$ W/K, independent of the acoustic velocity v . For $v = 10^4$ m/s, $\kappa_c^q(2D) \approx 0.78$ W/(m · K) and $\kappa_c^q(3D) \approx 2.7 \times 10^9$ W/(m² · K). The thermal conductances for multiple branches, for example, transverse and longitudinal, must be added appropriately to obtain the net conductance. Similar to the quantum limit of electrical contact resistances, practical thermal boundary resistances will be higher than the lower bounds of Eq. (11) due to phonon reflection at the boundary. A comparison with experimental values¹⁷ and practical interfacial effects such as non-unity transmission coefficients¹⁸ will be discussed in a separate work. By replacing the sound velocity with the speed of light ($v \rightarrow c$) in Eq. (11), one obtains the thermal boundary conductance when phonons convert to photons as alternate modes of interfacial thermal conductance (e.g., see Refs. 19 and 20).

Table I summarizes the results of this work. As a final point, we note that the combination $\frac{\kappa_c^q}{\sigma_c^q T^d}$ of temperature with the quantum limits of electrical contact conductance in the degenerate limit, and thermal boundary resistance, is independent of temperature and depends on fundamental parameters (q, k_b, h), on electronic band-structure parameters (g_s, g_v), the carrier density, and the phonon dispersion via the phonon velocity v . For 1D, this combination $\frac{\kappa_c^q}{\sigma_c^q T} = \frac{\pi^2}{3 g_s g_v} \cdot \frac{k_b^2}{q^2}$ appears similar to the Wiedemann–Franz law. This is surprising because the original Wiedemann–Franz law has thermal conductivity due to electrons (fermions) whereas here, it is due to phonons (bosons).

AUTHOR DECLARATIONS

Conflict of Interest

The authors have no conflicts to disclose.

Author Contributions

Alice Ho: Investigation (equal); Writing – review & editing (equal). **Jashan Singhal:** Investigation (supporting); Writing – review & editing (equal). **Deji Akinwande:** Investigation (supporting); Writing – review & editing (equal). **Huili G. Xing:** Investigation (supporting); Writing – review & editing (equal). **Debdeep Jena:** Conceptualization (equal); Data curation (equal); Formal analysis (equal); Investigation (lead); Project administration (equal); Writing – original draft (equal); Writing – review & editing (equal).

DATA AVAILABILITY

The data that support the findings of this study are available within the article.

REFERENCES

- J. Maassen, C. Jeong, A. Baraskar, M. Rodwell, and M. Lundstrom, “Full band calculations of the intrinsic lower limit of contact resistivity,” *Appl. Phys. Lett.* **102**, 111605 (2013).
- A. Baraskar, A. C. Gossard, and M. J. W. Rodwell, “Lower limits to metal-semiconductor contact resistance: Theoretical models and experimental data,” *J. Appl. Phys.* **114**, 154516 (2013).
- S. Datta, *Electronic Transport in Mesoscopic Systems* (Cambridge University Press, 1997).
- M. Lundstrom and C. Jeong, *Near-Equilibrium Transport: Fundamentals and Applications* (World Scientific Publishing Company, 2013), Vol. 2.
- C. Jeong, R. Kim, M. Luisier, S. Datta, and M. Lundstrom, “On landauer versus Boltzmann and full band versus effective mass evaluation of thermoelectric transport coefficients,” *J. Appl. Phys.* **107**, 023707 (2010).
- C. Jeong, S. Datta, and M. Lundstrom, “Full dispersion versus debye model evaluation of lattice thermal conductivity with a landauer approach,” *J. Appl. Phys.* **109**, 073718 (2011).
- R. Kim, S. Datta, and M. S. Lundstrom, “Influence of dimensionality on thermoelectric device performance,” *J. Appl. Phys.* **105**, 034506 (2009).
- J. Singhal and D. Jena, “Unified ballistic transport relation for anisotropic dispersions and generalized dimensions,” *Phys. Rev. Res.* **2**, 043413 (2020).
- The de Broglie wavelength λ_1 from Ref. 8 is: $\lambda_1 = h/\sqrt{2\pi m_1^* k_B T}$ for parabolic bands, and $\lambda_1 = hv_{F1}/(\sqrt{\pi} k_B T)$ for conical bands. $\lambda^d = \prod_{i=1}^d \lambda_i$, and the form λ_1/λ stands for $\lambda_1/(\prod_{i=1}^d \lambda_i)^{1/d}$ in d - dimensions. For example, for transport in one of the conduction band valleys of 3D silicon along the x direction, $\lambda_1/\lambda \equiv \lambda_x/(\lambda_x \lambda_y \lambda_z)^{1/3} = (m_x^* m_y^* m_z^*)^{1/6}/(m_x^*)^{1/2} = (m_y^* m_z^*/(m_x^*)^2)^{1/6}$.

- ¹⁰H.-S. P. Wong and D. Akinwande, *Carbon Nanotube and Graphene Device Physics* (Cambridge University Press, 2010).
- ¹¹D. Jena, K. Banerjee, and G. H. Xing, "Intimate contacts," *Nat. Mater.* **13**, 1076–1078 (2014).
- ¹²D. Akinwande, C. Biswas, and D. Jena, "The quantum limits of contact resistance and ballistic transport in 2D transistors," *Nat. Electron.* **8**, 96 (2025).
- ¹³D. Jena, *Quantum Physics of Semiconductor Materials and Devices* (Oxford University Press, 2022).
- ¹⁴E. T. Swartz and R. O. Pohl, "Thermal boundary resistance," *Rev. Mod. Phys.* **61**, 605 (1989).
- ¹⁵J. Chen, X. Xu, J. Zhou, and B. Li, "Interfacial thermal resistance: Past, present, and future," *Rev. Mod. Phys.* **94**, 025002 (2022).
- ¹⁶D. G. Cahill, W. K. Ford, K. E. Goodson, G. D. Mahan, A. Majumdar, H. J. Maris, R. Merlin, and S. R. Phillpot, "Nanoscale thermal transport," *J. Appl. Phys.* **93**, 793–818 (2003).
- ¹⁷K. Schwab, E. A. Henriksen, J. M. Worlock, and M. L. Roukes, "Measurement of the quantum of thermal conductance," *Nature* **404**, 974–977 (2000).
- ¹⁸G. Chen, *Nanoscale Energy Transport and Conversion: A Parallel Treatment of Electrons, Molecules, Phonons, and Photons* (Oxford University Press, 2005).
- ¹⁹Y. Guo, S. Tachikawa, S. Volz, M. Nomura, and J. Ordóñez-Miranda, "Quantum of thermal conductance of nanofilms due to surface-phonon polaritons," *Phys. Rev. B* **104**, L201407 (2021).
- ²⁰W. D. Hutchins, S. Zare, M. Habibzadeh, S. Edalatpour, and P. E. Hopkins, "Interfacial heat transport via evanescent radiation by hot electrons," *Phys. Rev. Lett.* **134**, 186302 (2025).